 doi:10.20944/preprints202203.0341.v1

Technical Note

Reflectance at Visible Wavelengths for Biological and Biochemical Characteristics of *Ocimum Basilicum* - Practicability of Colour Sensors for Plant Phenotyping

Tran Nam Trung [1], Rieke Keller [1], Trinh Quang Vinh [2]*, Tran Quoc Khanh [2] and Ralf Kaldenhoff [1]

[1] Department of Biology Applied Plant Sciences, Technical University Darmstadt, Schnittspahnstr. 10, 64287 Darmstadt, Germany;tran@bio.tu-darmstadt.de (T.N.T); Rieke.keller@stud.tu-darmstadt.de(R.Ke.);kaldenhoff@bio.tu-darmstadt.de (R.Ka.)
[2] Laboratory of Adaptive Lighting Systems and Visual Processing, Technical University of Darmstadt, Hochschulstr. 4a, 64289 Darmstadt, Germany; vinh@lichttechnik.tu-darmstadt.de (V.Q.T.); khanh@lichttechnik.tu-darmstadt.de (T.Q.K.)
* Correspondence: vinh@lichttechnik.tu-darmstadt.de (V.Q.T.); Tel.: +49 6151 16-22881

Abstract: Modern agriculture demands for comprehensive information about the plant itself. Conventional chemistry-based analytical methods - due to their low throughput and high associated cost - are no longer capable of providing these data. In recent years, remote reflectance-based characterization has developed as one of the most promising solutions for rapid assessments for plant attributes.

However, in many cases, expensive equipment is required because accurate quantifications need assessment of the full reflectance spectrum. We examined the versatility of visible colour sensors as reflectance measuring devices for biological / biochemical quantifications on sweet basil (Ocimum basilicum). Our results indicate for the wide potential of spectral colour sensors for quantitative determination of leaf phenolic compounds, flavonoids in particular, and non-invasive plant phenotyping in agricultural applications by low-cost sensors.

Keywords: Reflectance; Ocimum basilicum; Colour sensor; Phenotyping

1. Introduction

The emergence of modern precision agriculture (the so-called Agriculture 4.0) can be described as a fortuitous resonance of several technical and scientific advancements [1]. The complete sequencing of many plant genomes [2] and the rapid advances in genetic and metabolic engineering [3] lead to a deeper understanding of many biological and biochemical processes in plants and allow extensive manipulations of plant metabolic network. Soil-independent agricultural techniques such as hydroponics, aquaponics or aeroponics shift plant production from crop field to indoor plant factories. Here, a wide range of modern technologies control plant cultivation [4]. Automation [5], sensors [6], unmanned aerial vehicles (*UAV*) [7] and telecommunication techniques [8] enable a round-the-clock, real-time, multi-faceted monitoring and controlling of the production process. The quantum leap improvements in data science, artificial intelligence (*AI*) [9], computer processing power, speed and capacity of internet connectivity [10], enable the creation of sophisticated decision-making algorithms with minimal human intervention and unprecedented speed as well as precision that was just fantasy a few decades ago. These technologies demand on high quality and real time data. Thus, it is desirable to collect similar powerful methods to collect plant-related data for crop quality assessments.

 doi:10.20944/preprints202203.0341.v1

A variety of information can be achieved by analytical chemistry and molecular biology such as taste, flavours, ripeness, nutrient contents or small concentrations of numerous active compounds. While the methods themselves are very accurate and reliable, many are comparable slow, destructive, low-throughput and high cost both in terms of time and money. In addition, these often require well-equipped laboratories and skilful technicians. These drawbacks are increasingly evident considering the changes in agriculture in the first decades of the 21^{st} century. Recently, new approaches for the rapid quantification of plant biology and biochemistry parameter were established [11]. The method described herein employs the same principle known by farmers for thousands of years: reflectance-based measurements. When light reaches the surface of the plant, it can either be absorbed by plant tissues (absorbance), transmitted through the plant, and emerged on the other side (transmittance), or be reflected (reflectance). The degree of reflection depends on many factors including the light's wavelength, the angle of incidence and, importantly, the optical characteristics of plant tissues, which are in turn determined by its structural, biological, and biochemical properties (e.g., plant structure, surface roughness, tissue thickness and density, pigment contents) [12]. Therefore, it should be possible to receive information about plants from reflectance. The endeavour to elucidate this relationship gives rise to several new interdisciplinary research areas that were developed in recent years: remote sensing, hyperspectral imaging, optical contactless measurements or chemometrics [13].

Reflectance spectra of green leaf materials typically show low reflectance in blue and red regions, high for green wavelengths and strong for near-infrared (NIR) wavelengths [14]. Such features are attributed to the occurrence of two major plant pigments: chlorophylls and carotenoids. The concentration and ratio of these pigments serve as direct indicator of plant status. For example, low chlorophyll content indicates nitrogen deficiency, or a low chlorophyll/carotenoid ratio point to advanced senescence status. The first generation of reflectance-based plant analysis methods relies on a small number of wavelengths, from which information regarding the abundance of chlorophylls and carotenoids was estimated. The simplicity and robustness of this approach supports its popularity across a wide range of conditions [15]. The necessary sensors are readily available at low cost. Because the relationship between plant status and its pigment composition is established, interpretation of data is straightforward on one hand. On the other hand, only a limited number of plant traits can be characterized from pigment information only.

Most plant phenotypes do not correlate directly to reflectance. For example, many secondary metabolites are colourlessness and occur at low concentrations. They leave small, almost invisible reflectance footprints. Their production is generally independent from chlorophyll and carotenoid biosynthesis, thus there is no direct correlation with pigment contents. Their relationship to reflectance is therefore indirect with many intermediate factors. To predict such phenotypes, it is necessary to treat the connection between the complete reflectance spectra and the corresponding plant phenotypes as a black box and apply the principles of machine learning (*ML*) to build prediction models for the latter based on the former [16]. The measured reflectance spectra range between the visible (350 - 700 nm) and *NIR* regions (700 - 1100 nm) and often extends to shortwave infrared wavelengths (1100 - 2500 nm). The major advantage of this approach is that a priori knowledge regarding the relationship between reflectance and biological information is not required, therefore it is supposedly applicable for a much greater number of plant traits [17–19]. However, this approach is not without caveats because equipment for acquisitions of full spectra, such as spectrophotometer or hyperspectral camera, are expensive. Their cost and size were significantly reduced in recent years but still high enough to hold up widespread applications. We combine the positive features of the approaches, the utilization of *ML* algorithms with reflectance data collected from low-cost optical sensors. Advancement of sensor technology in recent years, which

Preprints (www.preprints.org) | NOT PEER-REVIEWED | Posted: 25 March 2022 doi:10.20944/preprints202203.0341.v1

resulted in a new generation of inexpensive, compact yet very powerful colour sensors make an application in agriculture possible.

A photodiode is the central element of a colour sensor. It consists of a semiconductor p-n junction device to convert an incident light-photon to electrical current. In general, this current is small and should be converted and amplified by an operational amplifier (*OPAM*). Subsequently, the analogue signal is converted into a digital one by an analogy-digital-converter (*ADC*). Besides these core and signal processing elements, optical filters are another essential element of colour sensors. Singular colour sensors - such as red, green, or blue filter detect the corresponding wavelengths of incident light. Simple singular colour sensors were generally utilized for monitoring the brightness levels of a specific colour. Often, these have limited specifications such as photodiodes or optical sensors from Hamamatsu [20]. Alternatively, several specific wavelength range filters can be combined for a more complex type of colour sensors called spectral sensors. Currently, very sophisticated spectral sensors with higher spectral wavelength channels such *AS7341* (8 visible optical channels, 3 extra channels of Clear, Flicker and *NIR*, size 3.1x2x1, 1.8 V and operate from -30° C to 70° C), *AS7343* (14 visible and *IR* channel, see Figure 1) or *AS7265x* (18 visible and *NIR* channels form 410 nm to 940 nm, 16-bit *ADC*s) are commercially available and can be integrated into cameras [21–25]. In recent years, the cost of colour sensors was reduced significantly, allowing a much wider range of applications including those in agriculture or horticulture [25].

A large potential for the application of such simple and tiny colour sensors in fully

Figure 1. *AS7343* provides a fast and accurate spectral measurement of incident light for crop cultivation (Source: Osram [25])

automated vertical farming facilities can be predicted. Effective contactless monitoring and controlling of the plant status is feasible and comparable to results from hyperspectral imaging, less expensive, though. With such systems, the growth, development, health status of plants and their interaction with environment conditions (temperature, humidity, light, water, and fertilizer) can be accurately and continuously measured and optimized. For practical applications, the performances of visible spectral sensors regarding stability, accurateness, and reliability are superior to those of far-infrared (*FIR*), *NIR* and ultraviolet (*UV*)-sensors. These sensors often suffer from high signal to noise ratios, degradation or input value shifting.

This work intends to provide a pre-feasibility study for potential applications in low-cost colour sensors to describe different biological and biochemical properties of plants. Therefore, the following restrictions were set:

This work intends to provide a pre-feasibility study for potential applications in low-

Preprints (www.preprints.org) | NOT PEER-REVIEWED | Posted: 25 March 2022 doi:10.20944/preprints202203.0341.v1

cost color sensors to describe different biological and biochemical properties of plants. Therefore, the following restrictions were set:

- Instead of a hyperspectral imaging camera, we collected reflectance data by taking many point measurements of the leaf upper side (adaxial) reflectance. It simulates the action of a colour sensor array.
- Unlike hyperspectral imaging cameras, colour sensors do not yield spatial information and cannot distinguish between plant substructures. Therefore, within one plant we could not distinguish between leaves with different leaf age or leaf position.
- Reflectance was measured in the visible wavelength range, i.e., from 380 nm to 800 nm, which is comparable to visible sensors in practical applications.
- Plants of different ages and from different cultivation conditions were analysed, reflecting the natural variation of plant-characteristics under these conditions.

We intend to determine which biological/ biochemical characteristics could still be reliably observed based on reflectance data and to evaluate the capability of low-cost colour sensors for phenotyping. As a model we chose sweet basil (*Ocimum basilicum*), a well-known herb used by humans for centuries. The basil system has several advantages: fast plant growth and simple cultivation; the plant is rich in secondary metabolic compounds with varying concentrations depending on age and growth conditions. Six plant parameters were chosen for analysis: specific leaf weight (SLW), total phenolic content (TPC), total flavonoid content (TFC) and the concentration of main pigments: chlorophyll a (ChA), chlorophyll b (ChB) and total carotenoids (CaT).

2. Materials and methods

2.1. Overview of the experimental plan

In total, 27 basil plants were used for the study. These were divided into three groups of nine plants each, three weeks after sowing. Each group was cultivated under three different light conditions: white light, red light, and blue/ red light mixture for another three weeks. After 5, 14 and 21 days from the onset of the experiments, three plants from each group were taken for analysis (Figures 2, 3). From each plant, ten leaf

Figure 2. Cultivation of sweet basil under three different light conditions

discs were excised for the determination of SLW as well as for reflectance measurements. The latter was performed on each leaf disc and the average of ten measurements was considered as representative for the whole plant. The rest of the leaf material was frozen in liquid nitrogen and treated for extraction of secondary coloured compounds.

Preprints (www.preprints.org) | NOT PEER-REVIEWED | Posted: 25 March 2022 doi:10.20944/preprints202203.0341.v1

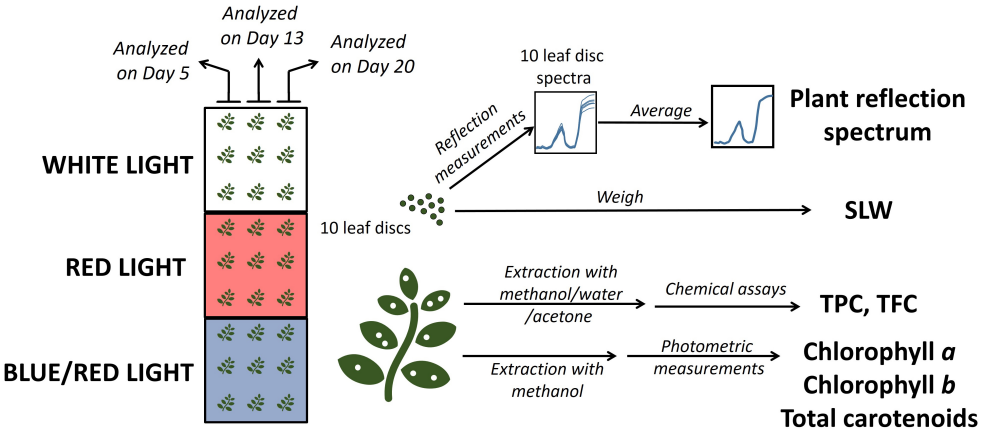

Figure 3. Overview of the experimental plan for determination of plant reflectance spectrum and biological and biochemical properties. *SLW* - Specific Leaf Weight; *TPC* - Total Phenolic Content; *TFC* - Total Flavonoid Content.

2.2. Plant cultivation

Ocimum basilicum (cultivar Genovese) was cultivated in soil pots (Fruhstorfer Erde Typ *T*, Hawita) under greenhouse conditions. Temperature was maintained between 19° C - 23° C with relative humidity at 50 - 60%. Three weeks after sowing, 27 young plants were transferred to a phytochamber (temperature 20°C, relative humidity 50%). Here, they were divided into three groups of nine plants each. These groups were further cultivated under three different light conditions: White-, red-, and blue / red -light combination (3/1). The day / night cycle was set at 16 h light: 8 h dark. Light intensity measured at the upper leaves was 100 $\mu mol/m^2 \cdot s$. The lights were adjusted daily to keep the light intensity constant as the plants grew. The spectra of the three lights used in the experiments are shown in Figure 4.

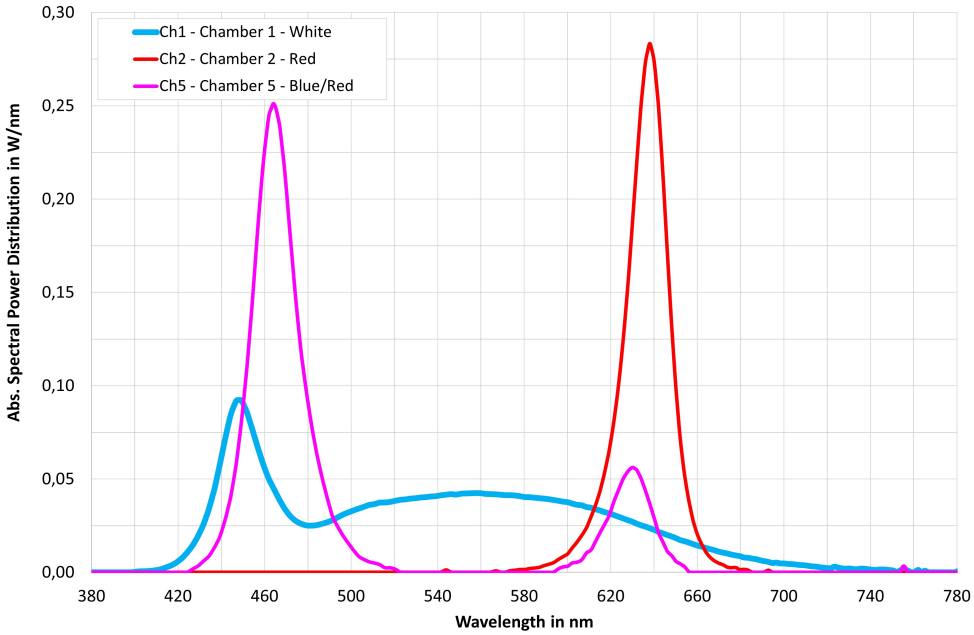

Figure 4. Absolut spectral power distributions of the three light conditions used in the experiments

 doi:10.20944/preprints202203.0341.v1

2.3. Analysis of plant's parameters

Determination of specific leaf weight (SLW): From each plant, ten leaf discs (0.95 cm in diameter) were randomly excised and immediately placed on a pre-weighed water agar plate (1%) to avoid desiccation (Figure 5). The agar plate weight was measured again and the difference (ΔW) estimated. SLW can be calculated with the following formula:

$$SLW\ [\frac{g}{cm^2}] = \frac{\text{Leaf weight}}{\text{Leaf surface}} = \frac{\Delta W}{10 \cdot \pi \cdot 0.95^2} \quad (1)$$

Within 10 minutes after excision, the leaf discs on the agar plate were used for reflectance

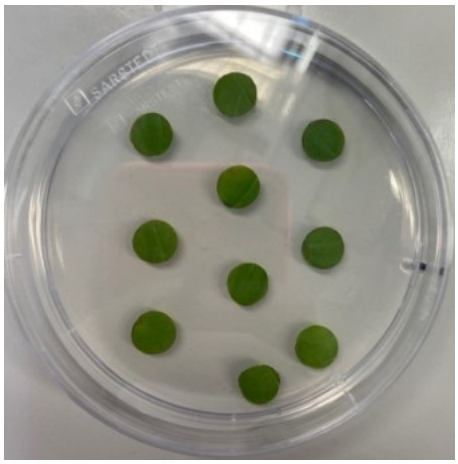

Figure 5. Leaf discs on agar plate

measurements.

2.4. Plant extracts

The remaining leaf material was frozen in liquid nitrogen and homogenized. Leaf powder weight was assessed. For extraction of phenolic compounds and flavonoids, 1 mL of methanol/water/acetone (60/30/10 v/v/v , freshly prepared) was added to each 250 mg of leaf material. The suspension was mixed vigorously and incubated at 4°C for 15 minutes. Subsequently, cell debris was removed by centrifugation at 4°C and 13,000 rpm for 10 minutes. The clear supernatant was transferred to a fresh tube. The extraction was repeated once more, and the supernatants were combined.

For extraction of photosynthetic pigments, 10 mL methanol was pre-treated with 150 mg calcium carbonate. To each 150 mg of frozen leaf powder, 1 mL pre-treated methanol was added, and the mixture centrifuged at 4°C and 13,000 rpm for 10 minutes. The extraction was repeated twice, and the supernatants were combined.

2.5. Quantification of total phenolic contents (TPC)

TPC of the methanol/water/acetone extract was determined with the Folin-Ciocalteu-Assay [26]. A calibration curve was created with standard solutions of gallic acid ranging from 250 to 750 mg/L. The total amount of phenolic content in the extract was determined from comparison to the calibration curve. TPC was calculated as the total amount of phenolic content per fresh weight unit.

$$TPC\ [\frac{\text{mg gallic acid equivalent}}{\text{g fresh weight}}] = \frac{\text{Total amount of phenolic compounds in extract}}{\text{Fresh weight used for extraction}} \quad (2)$$

Preprints (www.preprints.org) | NOT PEER-REVIEWED | Posted: 25 March 2022 doi:10.20944/preprints202203.0341.v1

2.6. Quantification of total flavonoid contents (TFC)

TFC of the methanol/water/acetone extract was determined by colorimetric measurement according to Zhishen et al. [27]. For calibration, solutions of (+)-catechin with concentrations ranging from 100 to 250 mg/L were used. TFC was calculated as the total amount of flavonoids per fresh weight unit.

$$TPC\ [\frac{\text{mg catechin equivalent}}{\text{g fresh weight}}] = \frac{\text{Total amount of flavonoids in extract}}{\text{Fresh weight used for extraction}} \tag{3}$$

2.7. Quantification of chlorophyll a, chlorophyll b and total carotenoids

The concentrations of chlorophyll a (ChA), chlorophyll b (ChB) and total carotenoids (CaT) were determined from the absorbance at 470 nm, 653 nm, and 666 nm [28] using the following equations:

$$ChA\ [mg/L] = 15.65 \cdot A_{666\ nm} - 7.34 \cdot A_{653\ nm} \tag{4}$$

$$ChB\ [mg/L] = 27.05 \cdot A_{653\ nm} - 11.21 \cdot A_{666\ nm} \tag{5}$$

$$CaT\ [mg/L] = \frac{1000 \cdot A_{470\ nm} - 2.86 \cdot [Chlorophylla] - 129.2 \cdot [Chlorophyllb]}{245} \tag{6}$$

Pigment content was calculated by dividing the pigment concentration in the extract by the fresh weight of plant material used for extraction.

2.8. Spectral reflectance – Measurement systems and spectral features

The measurement of leaf reflectance (Figure 6) requires a light source (LS), spectral camera (CS), white standard (WST) and leaves (L). The task of the light source LS is to generate a stable spectrum $S(\lambda)$that does not change regardless of the operating temperature or burning time. The standard spectral reflectance $WST(\lambda)$ of the white light standard, which consists of the $BaSO_4$ material, is approximately 1.0 across the full visible wavelength range (from 380 to 780 nm) according to the manufacturer. Initially, the spectral camera CS2000 measured the spectral production $S(\lambda) \cdot WST(\lambda)$ (Figure 6, left). Subsequently, the light source spectrum can be determined by Eq. 7.

$$S(\lambda) = \frac{S(\lambda) \cdot WST(\lambda) \text{ measured by CS}}{WST(\lambda) \text{ supplied by the manufacturer}} \tag{7}$$

Next, (Figure 6, right), white standard was replaced by a leaf (spectral reflectance $L(\lambda)$).

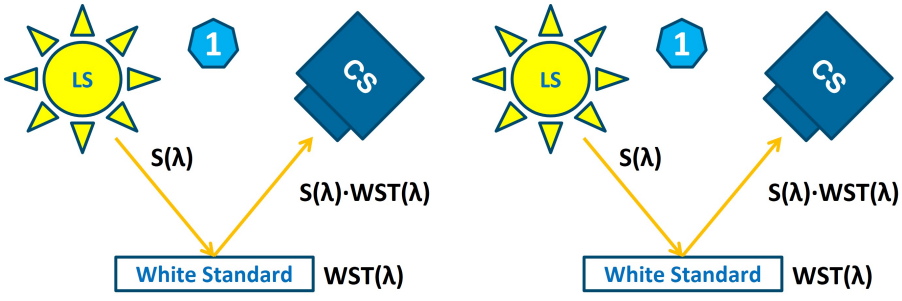

Figure 6. Measurement system and principle of spectral reflectance

The spectral production $S(\lambda) \cdot L(\lambda)$ was measured by a spectral camera CS. The light source spectrum (Eq. 7) and the spectral reflectance of the leaf was determined by Eq. 8.

$$L(\lambda) = \frac{S(\lambda) \cdot L(\lambda) \text{ measured by CS}}{S(\lambda) \text{ determined previously in Eq. 7}} \tag{8}$$

Preprints (www.preprints.org) | NOT PEER-REVIEWED | Posted: 25 March 2022 doi:10.20944/preprints202203.0341.v1

2.9. Plant parameter indicated by reflectance data

Mathematical description: to build a model, the equations 9 - 14 are introduced. The investigated parameters - TPC, TFC, ChA, ChB, CaT and SLW - are called generally Parameter X.

The spectral reflectance is represented by a matrix (26 x 401) with the matrix elements ($R_{i,j},\ j = 380 - 780,\ i = 1 - 26$). This matrix modified by a weighting function was also called weighting vector with the elements of W_1 to W_{780}.

The matrix multiplication of the spectral reflectance matrix and its weighting vector results in the intermediate vectors with the elements ($X_{interm.}, k,\ k = 1 - 26$), shown in Eq. 9. This intermediate vector was used for calculation of the prediction vector with linear equation as Eq. 10.

$$\begin{pmatrix} X_{\text{intern.},1} \\ \dots \\ X_{\text{intern.},26} \end{pmatrix} = \begin{pmatrix} R_{1,308} & \dots & R_{1,780} \\ \dots & \dots & \dots \\ R_{26,308} & \dots & R_{26,780} \end{pmatrix} \cdot \begin{pmatrix} W_1 \\ \dots \\ W_{780} \end{pmatrix} \tag{9}$$

$$\begin{pmatrix} X_{\text{predic.},1} \\ \dots \\ X_{\text{predic.},26} \end{pmatrix} = a \cdot \begin{pmatrix} X_{\text{intern.},1} \\ \dots \\ X_{\text{intern.},26} \end{pmatrix} + b \tag{10}$$

For next steps, the statistical parameters $ErrorVector$, Sum of Square Error (SSE), the average values between the experimental values and their mean values ($AVR.$) and R^2 are calculated like in Eq.11 to Eq. 14.

$$ErrorVector = \begin{pmatrix} X_{\text{predic.},1} \\ \dots \\ X_{\text{predic.},26} \end{pmatrix} - \begin{pmatrix} X_{\text{exper.},1} \\ \dots \\ X_{\text{exper.},26} \end{pmatrix} \tag{11}$$

$$SSE = \sum_{i}^{26} ErrorVector_i^2 \tag{12}$$

$$AVR. = \sum_{i}^{26} \left(X_{experi.,i} - \frac{\sum_{i}^{26} X_{experi.,i}}{26}\right)^2 \tag{13}$$

$$R^2 = 1 - \frac{SSE}{AVR.} \tag{14}$$

*** Optimization algorithm**: Subsequently, the optimization algorithm, was applied to determine parameter of the model. The optimization algorithm is described schematically in Figure 7. In our experiments, the plants were cultivated under different conditions to create a comprehensive experimental database for constructing the prediction models. Specifically, the following parameter: TPC, TFC, ChA, ChB, CaT and SLW of the cultivated plants were measured, processed, and determined to create the biological database (denoted Database 1 in Figure 7). The spectral (Section 2.8), represents Database 2 (Figure 7). The processing of Databases 2 with equations Eq. 9 to Eq. 14 results in the statistical values sum the square error (SSE) and R^2. Both the weighting elements of the weighting vector ($W_1 - W_{780}$ in Eq. 9) and linearity parameters (a and b in Eq. 10) are generated by the optimization algorithm. The optimization loop is implemented automatically and continuously until SSE is minimal and R^2 is maximal. The achieved results represent the weighting vectors and linearity parameters of the model.

Preprints (www.preprints.org) | NOT PEER-REVIEWED | Posted: 25 March 2022 doi:10.20944/preprints202203.0341.v1

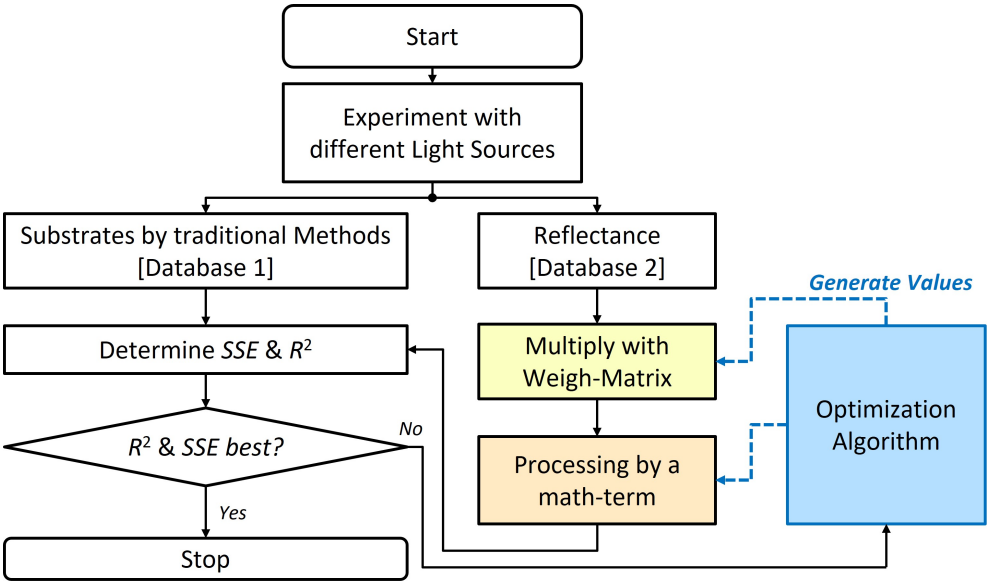

Figure 7. The schematic description of the synthesis optimization algorithm for prediction models

3. Results

3.1. Analysis of biological and biochemical parameter (Database 1)

We analysed six different parameters: TPC, TFC, ChA, ChB, CaT and SLW from 27 plants, which were cultivated under three different light conditions: white, red, and blue/red light; and harvested at three different days: day 5 (D_5), day 14 (D_{14}) and day 21 (D_{21}) after the onset of the experiment (Figure 8).

Our results indicate for significant variation of investigated plants, even in those from the same group (i.e., cultivated under the same light conditions and harvested at the same day). We performed the Kruskal-Wallis test to compare between plant groups categorized by either growth light conditions (White (W), Red (R) and Blue/Red (B/R)) or by age (i.e. the harvesting day Day 5 (D_5), 14 (D_{14}) and 21 (D_{21})). Our results (Table 1) indicate that there is no statistically significant difference ($p > 0.05$) of different light conditions. However, the age of the plants modified five out of the six investigated parameters significantly ($p < 0.05$).

Table 1: Kruskal–Wallis test performed on plants grouped by growth light conditions (White (W), Red (R) and Blue/Red (B/R)) or by age (harvesting on Day 5 (D_5), 14 (D_{14}) and 21 (D_{21})). SLW – Specific Leaf Weight; TPC – Total Phenolic Content; TFC – Total Flavonoid Content; ChA, ChB, CaT: chlorophyll a, chlorophyll b and total carotenoids contents

KRUSKAL-WALLIS TEST							
	Light condition groups ($W, R, B/R$)				Age groups (D_5, D_{14} & D_{21})		
	χ^2	df	p		χ^2	df	p
SLW	4.361	2	0.113	SLW	6.62	2	0.037
TPC	2.384	2	0.304	TPC	10.31	2	0.006
TFC	0.575	2	0.75	TFC	13.04	2	0.001
ChA	2.931	2	0.231	ChA	8.6	2	0.014
ChB	2.215	2	0.33	ChB	8.7	2	0.013
CaT	5.527	2	0.063	CaT	2.93	2	0.231

Preprints (www.preprints.org) | NOT PEER-REVIEWED | Posted: 25 March 2022 doi:10.20944/preprints202203.0341.v1

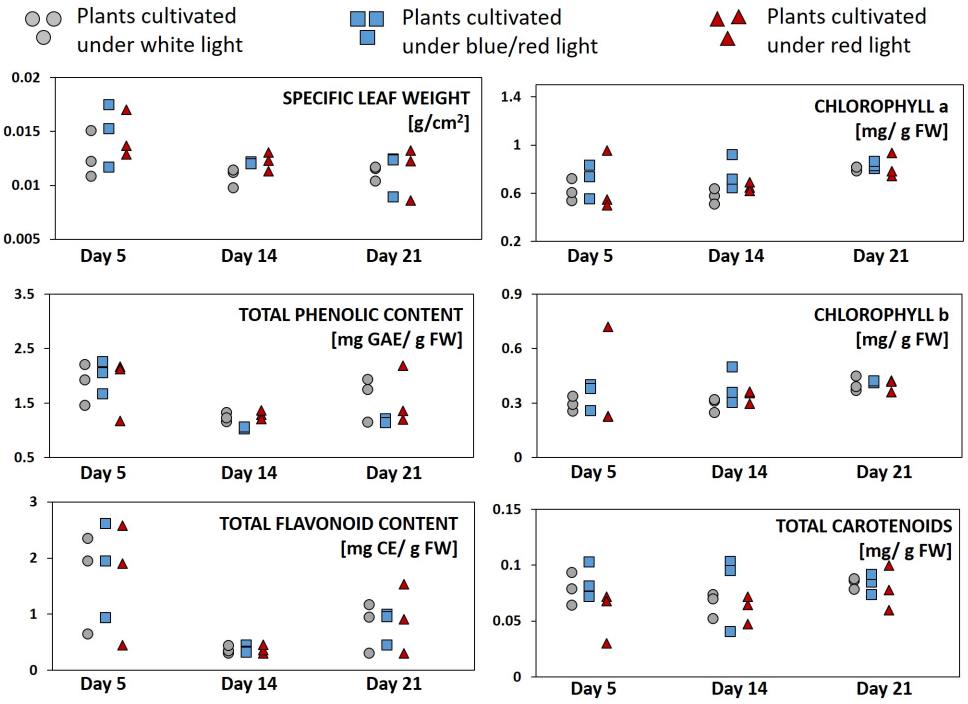

Figure 8. Analysis of six different plant parameters. Each symbol represents an individual plant. *GAE* – Gallic Acid Equivalent; *CE* – Catechin Equivalent; *FW* – Fresh Weight

3.2. Measurement of plant's reflectance (Database 2)

The spectral reflectance of leaves growing under different light conditions (red, blue/red and white) measured at different time points (5, 14 and 21 days after the start of the experiment) are depicted in Figure 9. Each plant is represented by 10 different point measurements, which were taken with 10 randomly excised leaf discs. All spectra share the same common pattern with a left slope at about 525 nm and a flatter right slope at about 600 nm, which meet at the maximal point at about 550 nm. Furthermore, a concave point at about 690 nm with an amplitude of about 10% for all leaves was observed. The region above 700 nm is characterized by a steep slope, which appears at about 710 nm and levels off from 720 nm to a plateau with an amplitude of about 60%. We also observed minor differences among 10 measured points. Such differences were highest after 5 days and then decreased. After 21 days, spectral reflectance was nearly constant.

3.3. Building the prediction models

The six investigated parameters - TPC, TFC, ChA, ChB, CaT and SLW - were optimized and synthesized with our optimization algorithm (Table 2). It can be concluded that only in the case of TPC and TFC, good correlations between experimental values and the prediction models based on the optimized weighting functions exist. In the four remaining cases of SLW, ChA, ChB and CaT, the correlation to the experimental values are weak ($R^2 = 0.209$ with SLW, $R^2 = 0.198$ with ChA and $R^2 = 0.151$ with ChB) or very weak ($R^2 = 0.021$ with CaT).

3.4. Correlations between reflectance and TPC/TLC

* **Total Phenolic Content** (TPC): optimization results of Total Phenolic Contents (TPC) are shown in detail in Figure 10. The upper subplot, depict the comparison between the experimentally determined and the predicted TPC shows a significant linear correlation. Statistical parameters R^2, dfe, $Adj. - R^2$ and $RMSE$ are 0.96179, 24, 0.9602

Preprints (www.preprints.org) | NOT PEER-REVIEWED | Posted: 25 March 2022 doi:10.20944/preprints202203.0341.v1

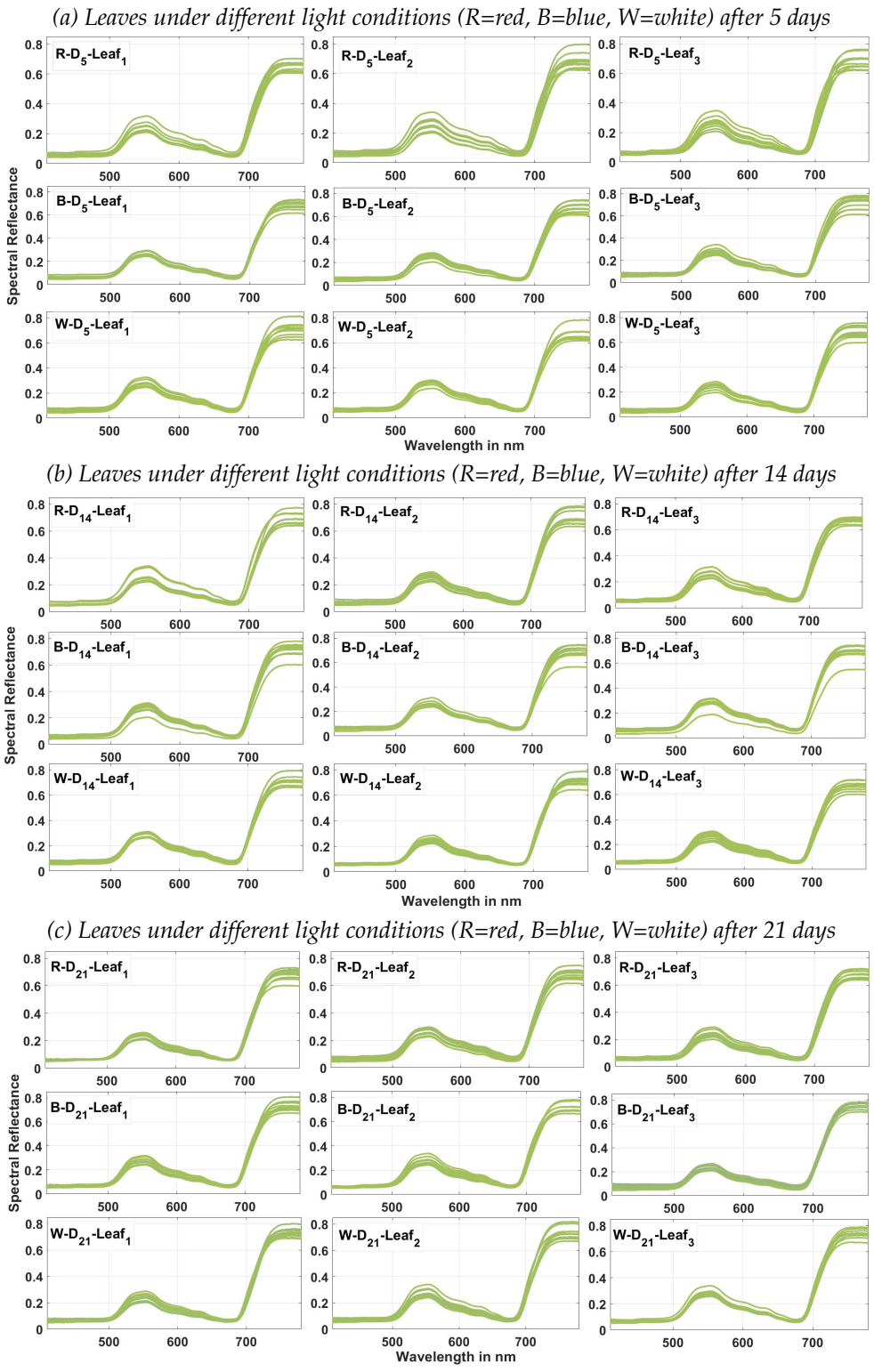

Figure 9. Spectral reflectance of leaves under different light sources after 5, 14 and 21 growth days

and 0.086236, respectively. Linearity parameters - $a_{eval.} = 0.9972$ and $b_{eval.} = 0.0034217$ – also compare favourably with the ideal ones $a_{eval.} = 1$ and $b_{eval.} = 0$. The residual plot (middle subplot) shows that all absolute residuals are under 0.2.

Of importance for the optimization algorithm is the weighting function. Only af-

Preprints (www.preprints.org) | NOT PEER-REVIEWED | Posted: 25 March 2022 doi:10.20944/preprints202203.0341.v1

Table 2: Optimization results of all parameter cases

Parameter	R^2	SSE	dfe	$Adj.R^2$	$RMSE$	$a_{eval.}$	$b_{eval.}$
Total Phenolic Content (TPC)	0.962	0.179	24	0.96	0.086	0.998	0.0034
Total Flavonoid Content (TFC)	0.876	1.886	25	0.88	0.274	1.004	0.0067
Specific Leaf Weight (SLW)	0.209	$8.8 \cdot 10^{-5}$	25	0.178	0.0019	0.998	0.209
Chlorophyll a (ChA)	0.151	0.45	25	0.12	0.13	7.296	4.516
Chlorophyll b (ChB)	0.198	0.211	25	0.166	0.092	1.061	0.028
Total Carotenoids (CaT)	0.021	0.064	25	-0.019	0.019	0.055	0.071

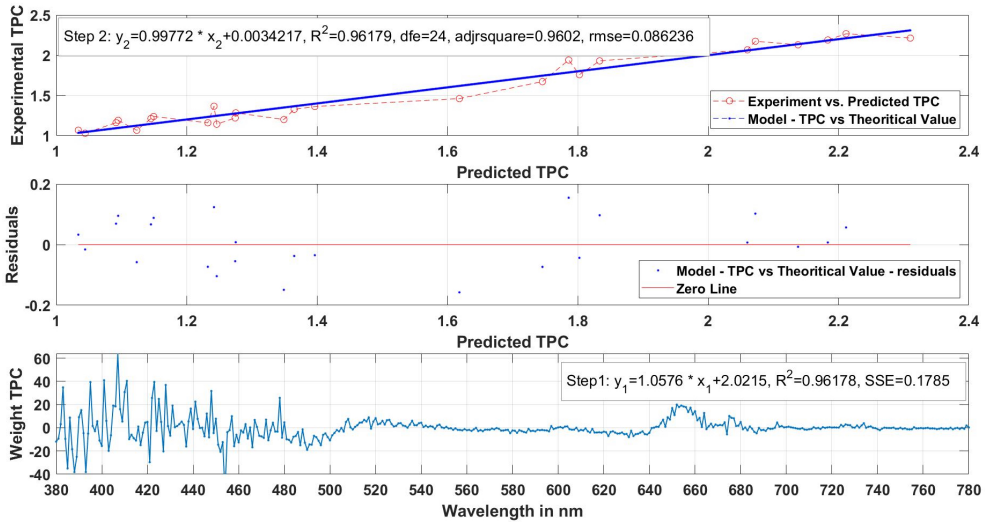

Figure 10. The prediction model, absolute residuals, and weighting function plots of the total phenolic content (TPC)

ter the weighting function has been optimized the other parameters of the equations Eq. 9 to Eq. 14 could be completed. The weighting function is displayed in the lower subplot. Here, the important wavelength ranges occur in the short wavelength range of from 380 nm to 500 nm and in the long wavelength range between 640 nm and 680 nm, which differs to the wavelength range of between 500 nm and 640 nm and from 680 nm to 780 nm remaining low and constant.

* **Total Flavonoid Content**: A comparable situation occurs in the case of TFC (Figure 11). The statistical parameter of the TFC model is somewhat inferior to the TPC ones but still very good with $R^2 = 0.87546$ and $SSE = 1.8862$. Absolute values are also larger. In the TFC weighting function, wavelength intensities stay relatively low and constant in regions between the 520 nm - 640 nm and between 700 nm - 780 nm. Like in the TPC model, the weighting function for TFC is dominated by two wavelength ranges of 380 nm - 520 nm and 640 nm - 700 nm. However, the patterns in these ranges are more complex.

4. Dicussion

In our experiment, large variations between plant individuals were observed even when they belong to the same light condition or age group. Plant-to-plant variations are an inherent and often problematic aspect in plant study since a large sample variance can easily mask the small but evident effects. In order to reduce the variance and thus

Preprints (www.preprints.org) | NOT PEER-REVIEWED | Posted: 25 March 2022 doi:10.20944/preprints202203.0341.v1

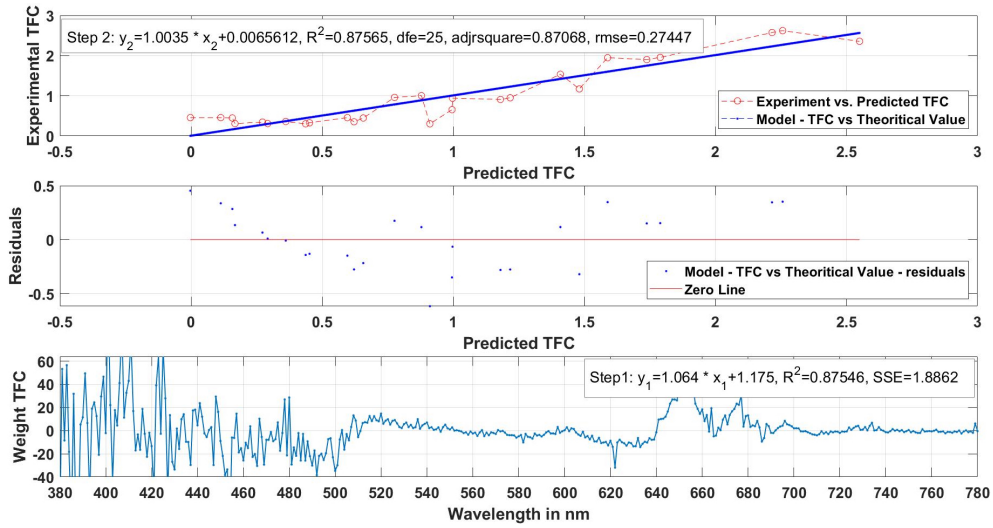

Figure 11. The prediction model, absolute residuals, and weighting function plots of the total flavonoid content (*TFC*)

enhance the power of the analysis, it is necessary to increase the sample size, i.e. to increase the number of investigated plants. Thanks to the low cost, high throughput and rapid rate of data acquisition associated with reflectance measurements, a much larger number of plants can be analysed by this method compared to the conventional chemistry-based analysis.

Accurate predictions of various biological and biochemical parameters of basil based on its reflectance properties have been achieved elsewhere [29,30]. However, the practical applicability of these findings is limited by the high cost of reflectance measuring equipment. As stated above, we applied several restrictions to our experiments to simulate the real life's limitations of colour sensors, including the mode of acquisition (point measurements instead of hyperspectral imaging) and wavelength range (visible region only). It is significant that even under these restrictions, we were able to establish good correlations between reflectance data and *TPC* respectively *TFC*. These two parameters represent the content of phenolic substances or flavonoids – two classes of secondary metabolites with important roles in the health-promoting effects as well as in the taste and flavour of sweet basil. Our results imply that the applications of colour sensors for quantification of *TPC*/*TFC* promises a reasonable probability of success and should be further investigated.

Both multi-channel spectral sensors and low-cost sensors can be utilized for such applications. The former, as seen in the examples of [21–25] can process many wavelength channels simultaneously. Using the established weighting functions (Figures 10, 11), the measured reflectance from these channels can be converted by simple mathematic transformations into the predicted *TPC*/*TFC* values. On other hand, low-cost sensors often have only one or a couple of photodiodes and some simple built-in electronic elements. They will require a different approach. We propose that in this case, the weighting functions should be physically processed by additional optical filters which are specifically tailored to match the features of the weighting functions. In the regions where wavelength intensities stay relatively low and constant (500 nm - 640 nm and 680 nm - 780 nm in case of *TPC* and 520 nm - 640 nm and 700 nm - 780 nm in case of *TFC*), simple optical filters will be sufficient. On the other hand, for the dominant regions (380 nm - 500 nm and 640 nm - 680 nm in case of *TPC* and 380 nm - 520 nm and 640 nm - 700 nm in case of *TFC*), sophisticated filter designs will be required.

 doi:10.20944/preprints202203.0341.v1

5. Conclusion

Our study confirms the applicability and scope of visible colour sensors for analysis and quantification of important plant properties In particular the content of valuable substances such as phenolic compounds and flavonoids (corresponding to Technical Readiness Level $TRL3$). Further work will be required to shift this concept into higher TRL levels. The establishment of the TPC and TFC weighting functions represents a significant step forward. Only with these weighting functions the successive processing techniques of colour sensors could be realized for the envisaged fully automated and accurately monitored/controlled vertical farming systems.

Author Contributions: Conceptualization: T.N.T, T.Q.V, T.Q.K and R.Ka; performance of experiments: T.N.T, R.Ke, T.Q.V; data analysis: T.N.T and T.Q.V; writing—original draft preparation, T.N.T and T.Q.V; writing—review and editing, T.N.T, T.Q.V, T.Q.K and R.Ka. All authors have read and agreed to the published version of the manuscript.

Funding: This work received no specific grant from any funding agency in the public, commercial, or not-for-profit sectors. The publication of the manuscript is supported by the Open Access Publishing Fund of the Technical University of Darmstadt.

Institutional Review Board Statement: Not applicable

Informed Consent Statement: Not applicable

Data Availability Statement: All data generated or analyzed to support the findings of the present study are included this article. The raw data can be obtained from the authors, upon reasonable request.

Conflicts of Interest: The authors declare no conflict of interest.

References

1. Araújo, S.O.; Peres, R.S.; Barata, J.; Lidon, F.; Ramalho, J.C. Characterising the agriculture 4.0 landscape—Emerging trends, challenges and opportunities. *Agronomy* **2021**, *11*, 667. doi:https://doi.org/10.3390/agronomy11040667.
2. Sun, Y.; Shang, L.; Zhu, Q.H.; Fan, L.; Guo, L. Twenty years of plant genome sequencing: Achievements and challenges. *Trends in Plant Science* **2021**. doi:https://doi.org/10.1016/j.tplants.2021.10.006.
3. Birchfield, A.S.; McIntosh, C.A. Metabolic engineering and synthetic biology of plant natural products–a minireview. *Current Plant Biology* **2020**, *24*, 100163. doi:https://doi.org/10.1016/j.cpb.2020.100163.
4. Ragaveena, S.; Shirly Edward, A.; Surendran, U. Smart controlled environment agriculture methods: a holistic review. *Reviews in Environmental Science and Bio/Technology* **2021**, *20*, 887–913. doi:https://doi.org/10.1007/s11157-021-09591-z.
5. Saleem, M.H.; Potgieter, J.; Arif, K.M. Automation in agriculture by machine and deep learning techniques: A review of recent developments. *Precision Agriculture* **2021**, *22*, 2053–2091. doi:https://doi.org/10.1007/s11119-021-09806-x.
6. Hassan, S.I.; Alam, M.M.; Illahi, U.; Al Ghamdi, M.A.; Almotiri, S.H.; Su'ud, M.M. A systematic review on monitoring and advanced control strategies in smart agriculture. *IEEE Access* **2021**, *9*, 32517–32548. doi:10.1109/ACCESS.2021.3057865.
7. Olson, D.; Anderson, J. Review on unmanned aerial vehicles, remote sensors, imagery processing, and their applications in agriculture. *Agronomy Journal* **2021**, *113*, 971–992. doi:10.1002/agj2.20595.
8. Tao, W.; Zhao, L.; Wang, G.; Liang, R. Review of the internet of things communication technologies in smart agriculture and challenges. *Computers and Electronics in Agriculture* **2021**, *189*, 106352. doi:10.1016/j.compag.2021.106352.
9. Benos, L.; Tagarakis, A.C.; Dolias, G.; Berruto, R.; Kateris, D.; Bochtis, D. Machine learning in agriculture: A comprehensive updated review. *Sensors* **2021**, *21*, 3758. doi:10.3390/s21113758.
10. Osinga, S.A.; Paudel, D.; Mouzakitis, S.A.; Athanasiadis, I.N. Big data in agriculture: Between opportunity and solution. *Agricultural Systems* **2022**, *195*, 103298. doi:10.1016/j.agsy.2021.103298.
11. Kolhar, S.; Jagtap, J. Plant trait estimation and classification studies in plant phenotyping using machine vision–A review. *Information Processing in Agriculture* **2021**. doi:10.1016/j.inpa.2021.02.006.
12. Grzybowski, M.; Wijewardane, N.K.; Atefi, A.; Ge, Y.; Schnable, J.C. Hyperspectral reflectance-based phenotyping for quantitative genetics in crops: Progress and challenges. *Plant Communications* **2021**, *2*, 100209. doi:https://doi.org/10.1016/j.xplc.2021.100209.
13. Houhou, R.; Bocklitz, T. Trends in artificial intelligence, machine learning, and chemometrics applied to chemical data. *Analytical Science Advances* **2021**, *2*, 128–141. doi:10.1002/ansa.202000162.
14. Su, W.H.; Sun, D.W. Multispectral imaging for plant food quality analysis and visualization. *Comprehensive Reviews in Food Science and Food Safety* **2018**, *17*, 220–239. doi:10.1111/1541-4337.12317.

15. Mulla, D.J. Twenty five years of remote sensing in precision agriculture: Key advances and remaining knowledge gaps. *Biosystems Engineering* **2013**, *114*, 358–371. Special Issue: Sensing Technologies for Sustainable Agriculture, doi:10.1016/j.biosystemseng.2012.08.009.
16. Dale, L.M.; Thewis, A.; Boudry, C.; Rotar, I.; Dardenne, P.; Baeten, V.; Pierna, J.A.F. Hyperspectral imaging applications in agriculture and agro-food product quality and safety control: A review. *Applied Spectroscopy Reviews* **2013**, *48*, 142–159. doi:10.1080/05704928.2012.705800.
17. Sarić, R.; Nguyen, V.D.; Burge, T.; Berkowitz, O.; Trtílek, M.; Whelan, J.; Lewsey, M.G.; Čustović, E. Applications of hyperspectral imaging in plant phenotyping. *Trends in Plant Science* **2022**. doi:10.1016/j.tplants.2021.12.003.
18. Centner, V.; Massart, D.L.; de Noord, O.E.; de Jong, S.; Vandeginste, B.M.; Sterna, C. Elimination of uninformative variables for multivariate calibration. *Analytical chemistry* **1996**, *68*, 3851–3858. doi:10.1021/ac960321m.
19. Carlini, P.; Massantini, R.; Mencarelli, F. Vis-NIR measurement of soluble solids in cherry and apricot by PLS regression and wavelength selection. *Journal of Agricultural and Food Chemistry* **2000**, *48*, 5236–5242. doi:10.1021/jf000408f.
20. Hamamatsu. Optical sensors. https://www.hamamatsu.com/eu/en/product/optical-sensors.html?nfxsid=CjwKCAiAsNKQBhAPEiwAB-I5zQAzlfPg93WQ8oNYea-Hj33gB4wZ9bqv1ZtYV2578o6as_DKO-wUNBoCEe0QAvD_BwE&gclid=CjwKCAiAsNKQBhAPEiwAB-I5zQAzlfPg93WQ8oNYea-Hj33gB4wZ9bqv1ZtYV2578o6as_DKO-wUNBoCEe0QAvD_BwE, 2022. [Online; March 23, 2022].
21. Osram, A. Spectral Sensing. https://ams.com/en/spectral-sensing, 2022. [Online; March 23, 2022].
22. AMS. S7341 – 11-Channel Spectral Color Sensor. https://ams.com/en/as7341, 2022. [Online; March 23, 2022].
23. Osram, A. ams OSRAM AS7265x Smart Spectral Sensors. https://www.mouser.de/new/ams-osram/ams-as7265x-sensors/, 2022. [Online; March 23, 2022].
24. IMEC. Explore the potential of hyperspectral imaging. https://www.imechyperspectral.com/en/explore-potential-hyperspectral-imaging?gclid=CjwKCAiAsNKQBhAPEiwAB-I5zQwrh1xNdVrAUolD0TuKi4VlfQZjBfXU_bmZj_5yc1Elhp4MFXvTmBoCdPgQAvD_BwE, 2022. [Online; March 23, 2022].
25. Osram, A. New AS7343 multi-spectral sensor adds XYZ technology to increase speed and accuracy of color measurements. https://ams.com/-/as7343?utm_source=linkedin&utm_medium=social&utm_campaign=Horticulture&utm_term=PR&utm_content=card, 2022. [Online; March 23, 2022].
26. Waterhouse, A.L. Determination of Total Phenolics. Current Protocols in Food Analytical Chemistry. *John Wiley & Son, Inc.* **2002**, *6*, I1–1.
27. Zhishen, J.; Mengcheng, T.; Jianming, W. The determination of flavonoid contents in mulberry and their scavenging effects on superoxide radicals. *Food Chemistry* **1999**, *64*, 555–559. doi:https://doi.org/10.1016/S0308-8146(98)00102-2.
28. Lichtenthaler, H.K. Chlorophylls and carotenoids: Pigments of photosynthetic biomembranes. In *Plant Cell Membranes*; Academic Press, 1987; Vol. 148, *Methods in Enzymology*, pp. 350–382. doi:https://doi.org/10.1016/0076-6879(87)48036-1.
29. Schulz, H.; Schrader, B.; Quilitzsch, R.; Pfeffer, S.; Krüger, H. Rapid classification of basil chemotypes by various vibrational spectroscopy methods. *Journal of Agricultural and Food Chemistry* **2003**, *51*, 2475–2481. doi:10.1021/jf021139r.
30. Lazarević, B.; Šatović, Z.; Nimac, A.; Vidak, M.; Gunjača, J.; Politeo, O.; Carović-Stanko, K. Application of phenotyping methods in detection of drought and salinity stress in basil (Ocimum basilicum L.). *Frontiers in Plant Science* **2021**, *12*, 174. doi:https://doi.org/10.3389/fpls.2021.629441.